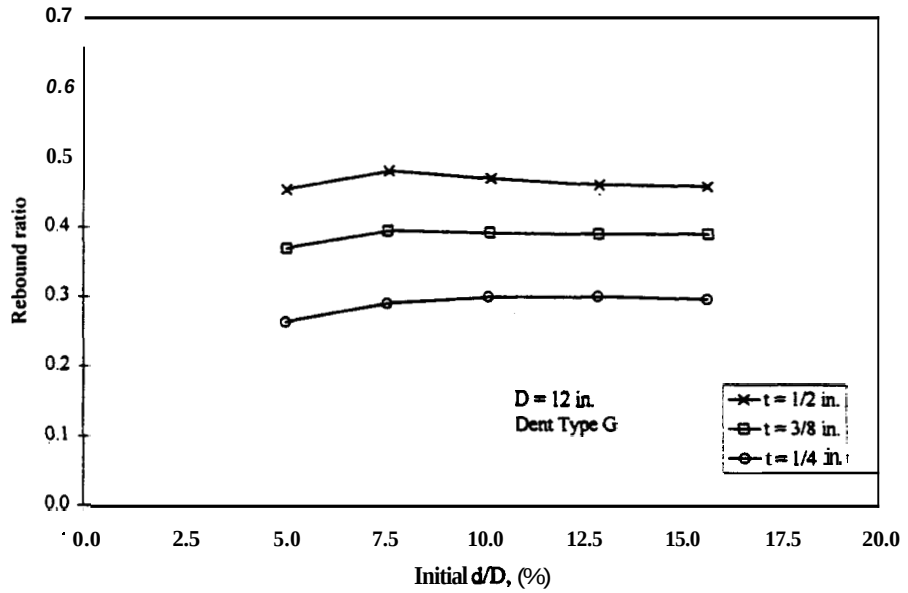

Figure 4-52: Rebound Ratio **vs.** initial **dent depth for** all Type **G dents in 12 in. pipes.**

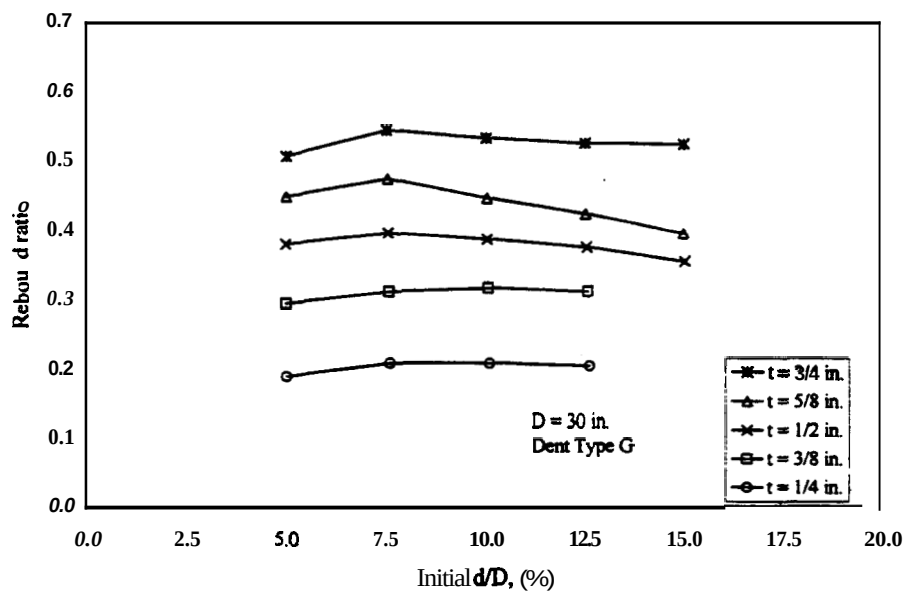

Figure 4-53: Rebound Ratio vs. initial dent depth for all Type **G dents in 30 in. pipes.**

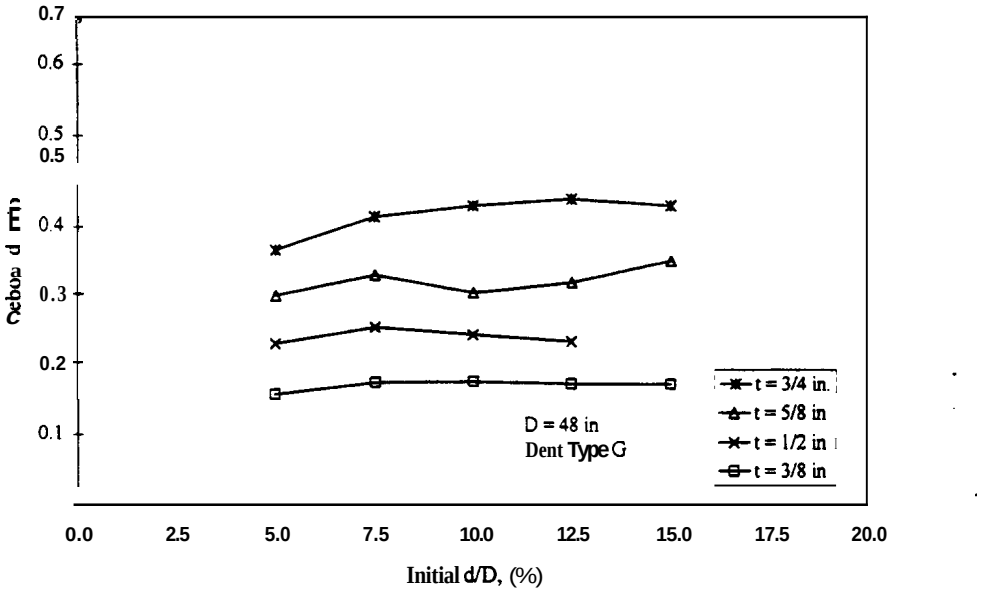

Figure 4-54: Rebound Ratio vs. initial dent depth for all Type **G dents in 48 in. pipes.**

Table 4-9: Rebound Ratios for Type *G* **dents.**

Thickness, *t* (in.)	Diameter, *D* (in.)					
	Grade 60X			Grade B		
	12	18	24	30	36	48
0.250	0.30	0.24	0.19	0.21	0.16	-----
0.375	0.39	0.33	0.28	0.32	0.26	0.18
0.500	0.47	0.40	0.34	0.39	0.34	0.24
0.625	-----	-----	0.40	0.45	0.40	0.31
0.750	-----	-----	-----	0.53	0.50	0.43

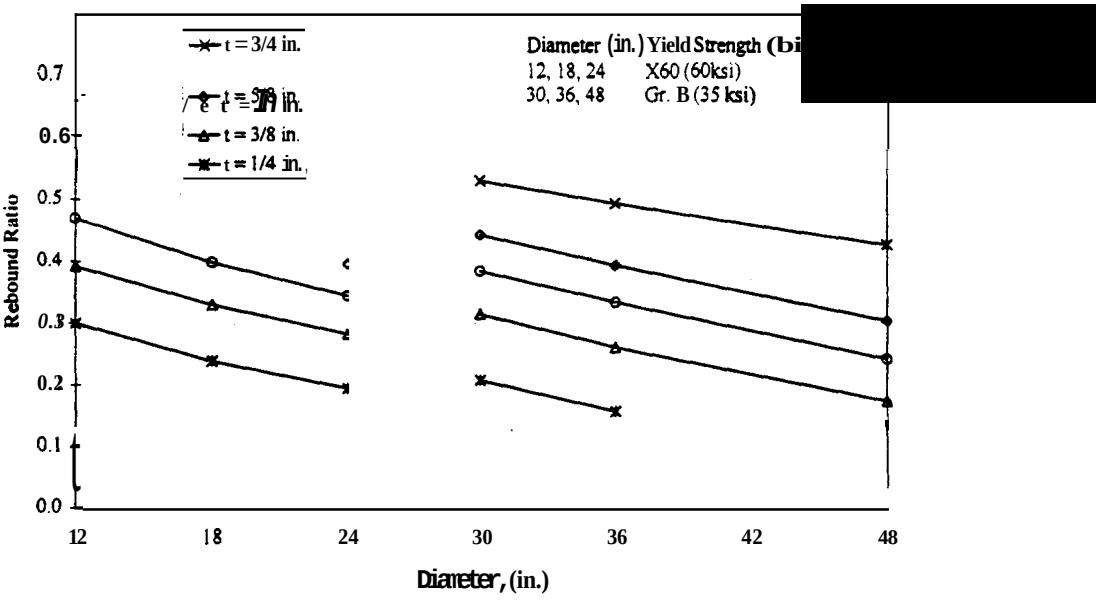

Figure 4-55: Rebound Ratio of **Type** G dents.

4.4.6 Dent Type H Rebound Behavior

Several models were dented with the **Type** H indenter to see how a change in indenter width influences the behavior of dents when compared to dents fiom the **Type** G indenter. The diameter of the **Type** H indenter is 8 in. as compared to 1 in. for the **Type** G indenter. Both dent types have an indenter length of 12 in. Modeling was performed on pipe diameters of 12 in., 18 in., and 48 in.

The length of the dent gives **Type** H dents the characteristic bulge found with long dent behavior. Thus, significant rebound occurs fiom initial and final rebound. Figure **4-56** shows the shape of **Type** H dents at indentation for Pipe **18-3.** The length of the contact region for the *Type* H dent in Fig. **4-56** is 4 in. This results in a total contact length of 8 in. since the end radius of the indenter is included in the overall length (Fig. 4-1). The similar graph given in Fig. **4-56** for a Type G dent shows that the contact length is 10 in. (Fig. **4-44).** The total length of the cylindrical portion of the **Type** G dent is 10 in. (Fig. **4-1).** The overall lengths of the Type G and H indenters are the same, but the contact length each has during indentation is different. The

Type H dent has a shorter contact length. Thus, comparing Type G and H dents based strictly on dent width is not possible since the indenter lengths are different. The Type G dent should be more susceptible to long dent behavior due to the increased dent length. The two dent types can be compared based on width, but the indenter length parameter is not constant for the comparison.

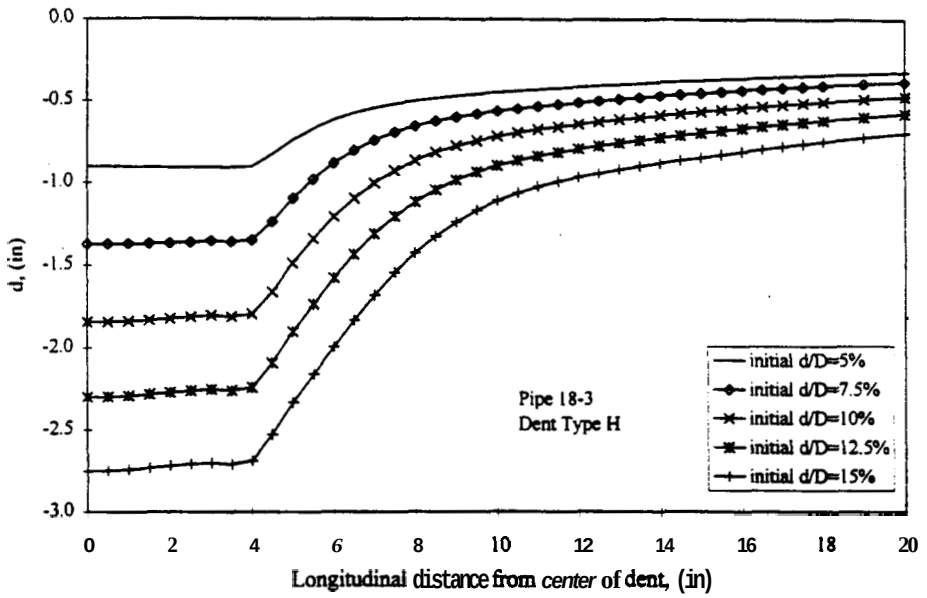

Figure 4-56: Type H dent depth at indentation for Pipe 18-3.

The dent shape after initial and final rebound is given in Figs. 4-57 and 4-58. As with Type A and G dents, the bulging behavior causes the final depths at the center of the dent to have similar values for dents of different initial depth. As with other long dents, depth measurements are recorded at the end of the contact region. The final rebound dent shape longitudinally is similar to that of the Type G dent (Fig. 4-46).

Increasing the diameter reduces the bulging behavior for Type H dents. The dent shape for Type H dents in Pipe 48-6 is given in Fig. 4-59. The shallower depths have slight bulging behavior, whereas the deeper dents to not develop bulges due to the increase in dent stiffness from the increased dent depth. The behavior of the Type H dent in Pipe 48-6 is similar to behavior of the Type G dent for the same pipe (Fig. 4-48).

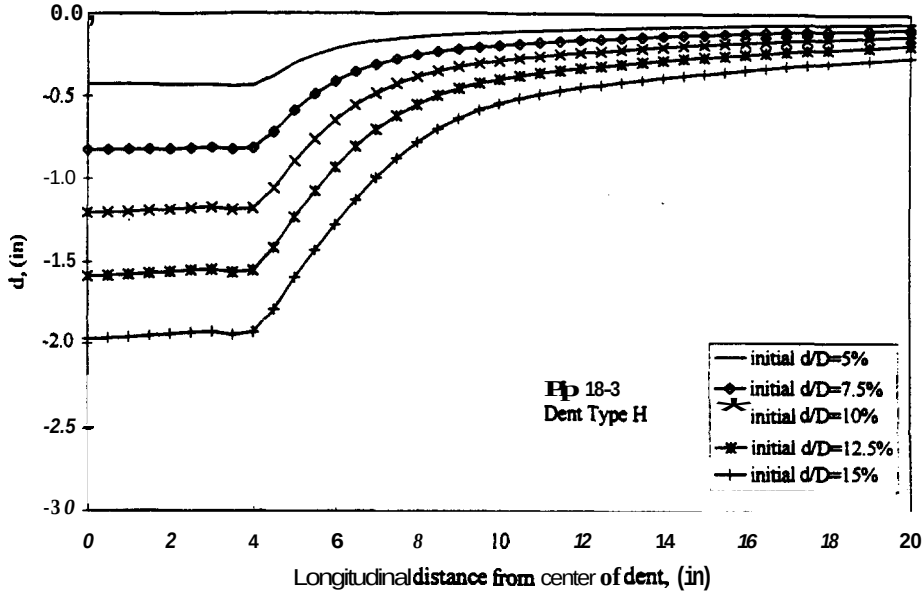

Figure 4-57: Type H **dent depth after** initial **rebound for Pipe** 18-3.

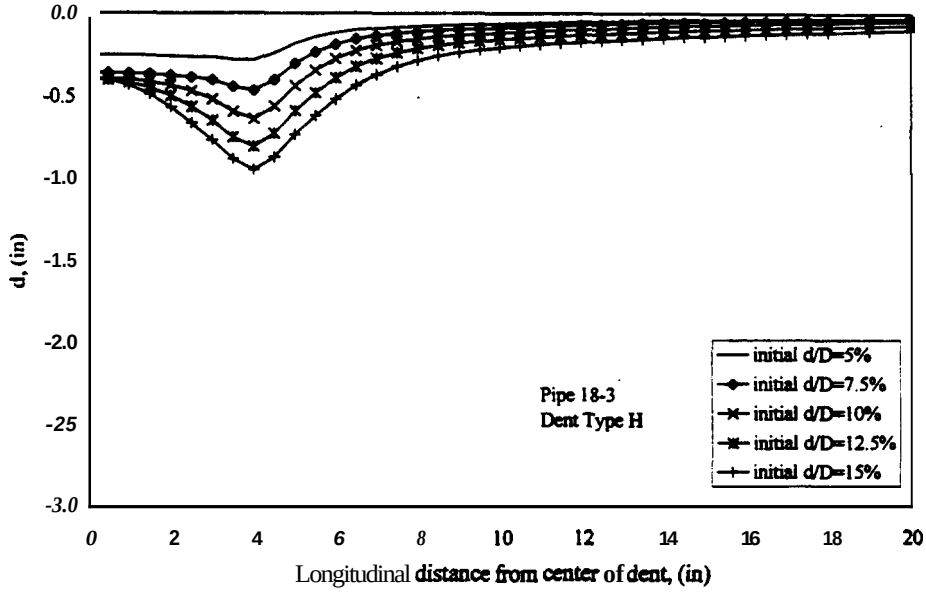

Figure 4-58: Type H dent depth after final rebound for Pipe 18-3.

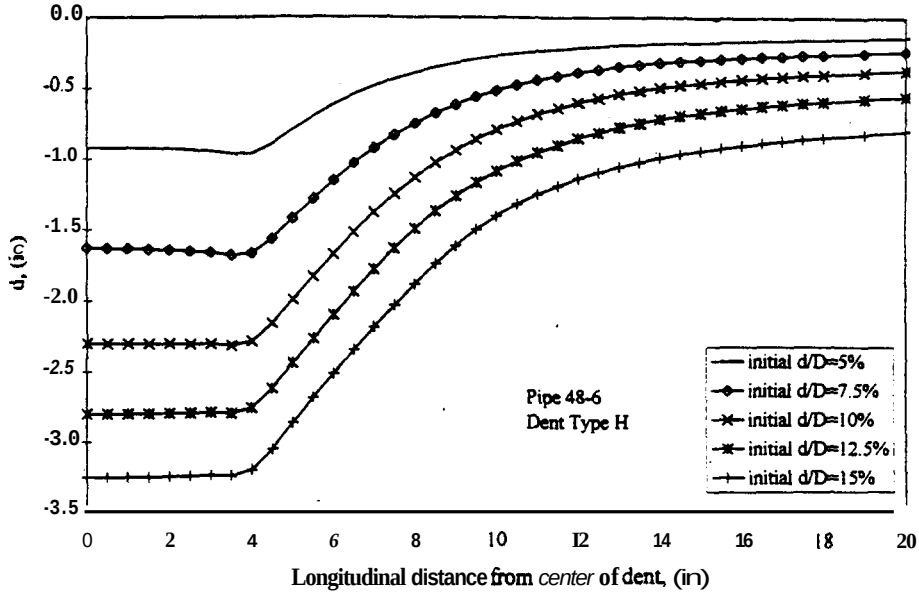

Figure 4-59: Type H dent depth after final rebound for Pipe 48-6.

The difference in rebound shapes between Type G and H dents is minimal. Comparisons of the final rebound dent shapes of the pipe cross section for the two dent types is similar. Displacement of the cross section was only recorded along node set RING1. Thus, the shapes of the cross section for Type G and H dents for Pipe 18-3 will be similar at the RING1 cross section due to the bulging behavior of the dents. Neither dent type had bulging behavior for Pipe 48-6. Thus, comparisons between the shapes of the cross section for RING1 should be similar for cross sections throughout the length of the contact region. The dent Type H displaced cross section after final rebound for Pipe 48-6 is given in Fig. 4-60. The corresponding displaced cross section for dent Type G is given in Fig. 4-61. The displaced shapes are very similar. Thus, the increase in width of the cylindrical indenter has little influence on the rebound characteristics of dents.

The relationship of initial and final dent depths of Type H dents has the same correlation as the other longitudinal dents types. The Rebound Ratio is constant with respect to dent depth as shown in Fig. 4-62 for 18 in. diameter pipes with Type H dents. Rebound Ratio data for the three diameters of Type H dents modeled is given in Table 4-10.

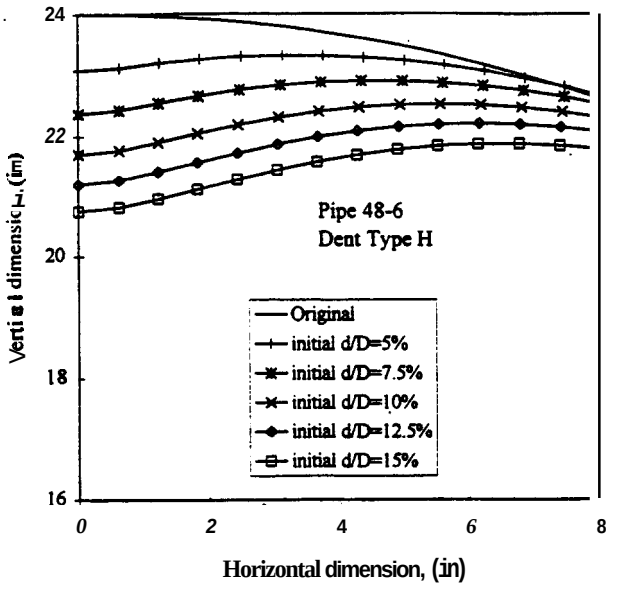

Figure 4-60: Type H dent displaced cross section after final rebound for Pipe 48-6.

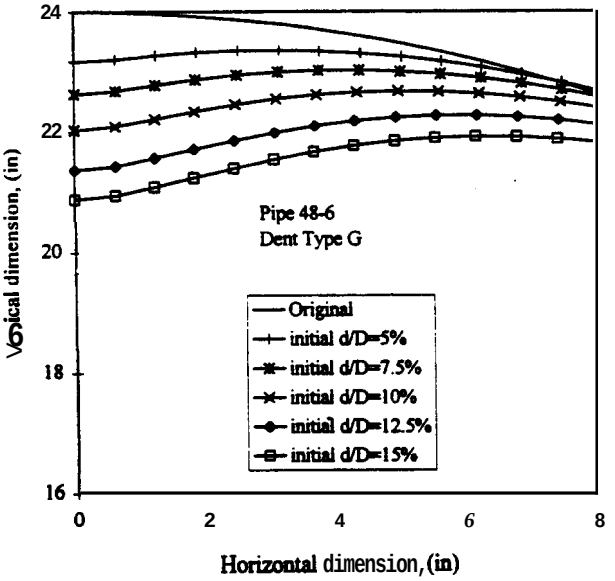

Figure 4-61: Type G dent displaced cross Section after final rebound for Pipe 48-6.

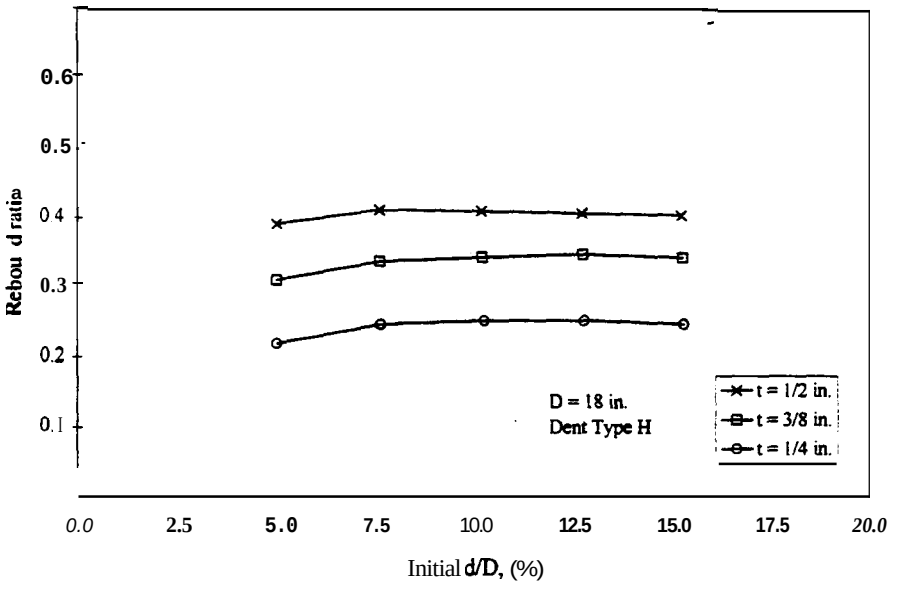

Figure 4-62: Rebound Ratio vs. initial dent depth for all Type H dents in 18 in. pipes.

Table 4-10: Rebound Ratios for Type H dents.

Thickness, *t* (in.)	Diameter, *D* (in.)					
	Grade 60X			Grade B		
	12	18	24	30	36	48
0.250	0.33	0.25	-----	-----	-----	-----
0.375	0.43	0.34	-----	-----	-----	0.18
0.500	0.50	0.41	-----	-----	-----	0.26
0.625	—	—	—	—	-----	0.40
0.750	-----	-----	-----	-----	-----	0.48

4.5 STRESS BEHAVIOR OF UNRESTRAINED LONGITUDINAL DENTS

4.5.1 Introduction

The stress distributions in and around longitudinal dents were investigated. Transverse and longitudinal stress distributions were recorded for the inside and outside surfaces along node set TOP. All fatigue cracks that developed in the various dent types of the experimental program initiated along the line representing node set TOP. Type A dents developed longitudinal cracks in the dent contact region. Type BH dents developed longitudinal periphery cracks on both sides of the dent collinear with the contact region in the longitudinal direction. Crack initiation occurred on the outside surface for both cases (no cracks initiated on the inside surface). Thus, this study will concentrate on the distribution of the outside surface transverse stress for node set TOP. Stress contour plots of the pipe model were created to better understand the stress distributions of dented pipes. The objectives of the stress analysis are to:

- Determine locations of possible fatigue failure for the various parameters
- Understand the failure modes found in the experimental program
- Correlate stress behavior with rebound behavior
- Collect fatigue stress range data for fatigue life prediction
- Understand the influence of bending and membrane stresses on the stress behavior

As with the rebound behavior of unrestrained longitudinal dents discussed in Sec. 4.4, the stress behavior is organized by dent type.

The experimental program had fatigue failures corresponding to failure Modes 1 and 2. The primary parameter found to influence failure mode was the dent length. The change in pipe dimensions was also found to influence the mode of failure. The larger diameter test specimens with Type A dents did not develop the bulging rebound behavior characteristic of long dent behavior. Increasing diameter and increasing dent depth of Type A dents was found to transition the failure mode from long dent behavior to short dent behavior. The finite element modeling expands the study of transition of failure mode due to the wide range of pipe sizes modeled which was not feasible with experimental testing.

Fatigue stress range data was collected in an attempt to develop stress concentration relationships for fatigue life prediction. The fatigue life prediction of dents is complex due to the influence of contact damage from indentation and the changes of rebound characteristics associated with different dent or pipe parameters.

Internal pressurization causes membrane and bending stresses to develop in dents. The design pressure of a pipeline is based on membrane stress. The geometry and rebound characteristics of dents can change the membrane stress behavior. The flexibility of a dent can cause an increase in membrane stress in the periphery of dents as the membrane stress flows around the flexible dent region into the periphery of the dent region which has higher stiffhess. Study of this stress behavior illustrates the influence of membrane stress on the fatigue behavior of dents. The simple model shown in Fig. 4-63 shows the increased flexibility of the dent relative to the undented pipe wall. Strain compatibility causes the periphery to have a stress concentration from the membrane hoop stress.

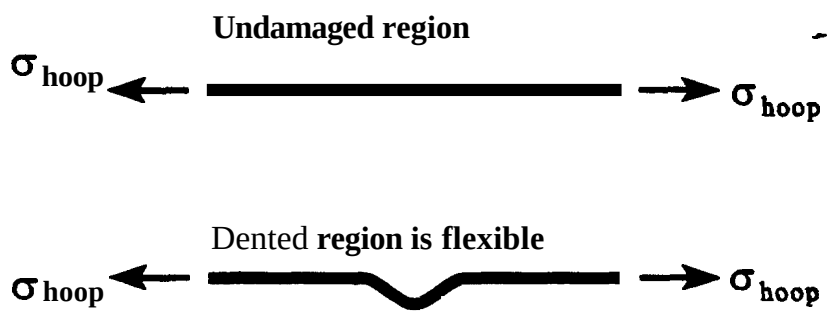

Figure 4-63: Membrane hoop stress in dented region and periphery.

Localized bending stresses develop in and around dents due to the rebound behavior associated with pressure cycling. Rebound of unrestrained dents causes tensile bending stress to develop on the outside surface of the dented region. Compressive bending stress develops on the inside surface. (These stresses are opposite to those that develop during denting.) The superposition of tensile membrane stress with tensile bending stress causes fatigue cracks to initiate on the outside pipe surface. An increase in slenderness corresponds to an increase in dent flexibility which causes an increase in the bending stress. Thus, bending stress has more

influence on the transverse stress behavior with increasing slenderness.

The viewpoint used to display contour plots is given in Fig. 4-64. This viewpoint is directly above the pipe model in the direction of indentation. The model represents one fourth of a pipe due to the planes of symmetry. Node sets TOP and RING1 are given as well as the transverse and longitudinal directions of the pipe. In contour plots, a transparent view of the indenter will be displayed to give a reference of the stress plots to the indenter geometry. The transparent indenter is only in contact with the pipe mesh during the indentation step. The indenter is removed fiom the pipe mesh in the step of elastic rebound such that it is not in contact and distributes zero force during pressurization.

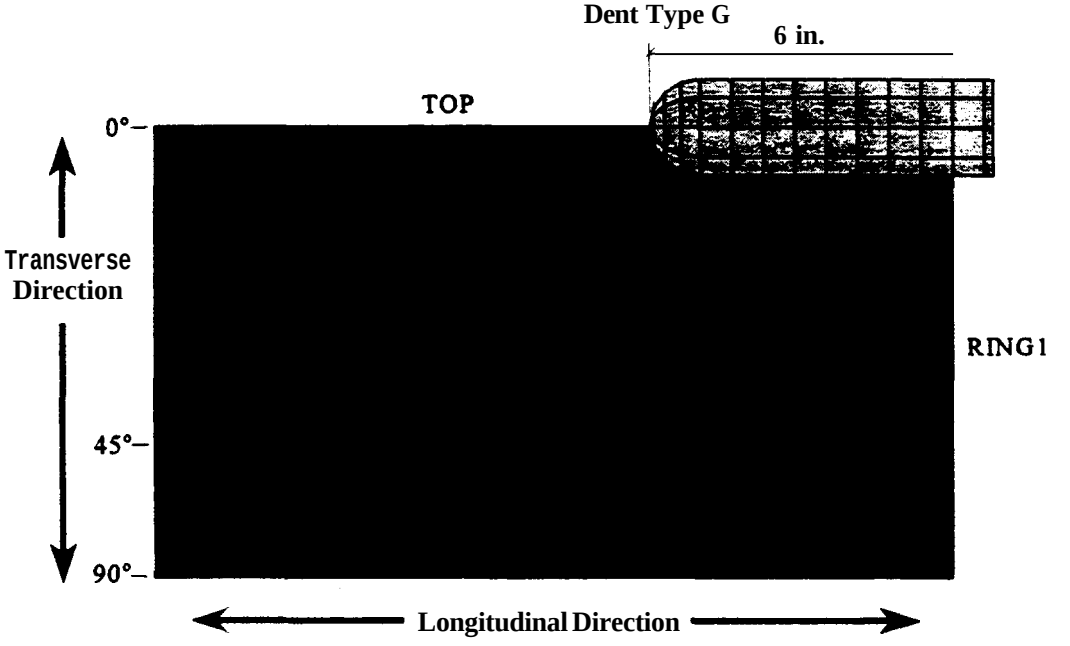

Figure 4-64: Model plot for clarification of contour plot viewpoint.

4.5.2 Dent Type A Stress Behavior

Indentation causes high compressive stresses on the outside surface in and around the dent contact region. While high tensile stresses develop on the inside surface of the dented region. This is evident for both the transverse and longitudinal stresses. Figure 4-65 shows a

plot of outside surface transverse stress from indentation through final rebound for a 10 percent *d/D* Type A dent in Pipe 18-3. The final residual dent depth is graphed to show stress behavior with respect to dent location. There was zero internal pressure during indentation and initial rebound. At indentation, the outside surface transverse stress is in a state of high compressive stress in the contact region. Removal of the indenter force allows elastic rebound. After initial rebound, the stress level at the contact region is tensile in the elastic range. The highest stress level is located in the dent periphery. Pressurization causes both elastic and plastic rebound. At this stage, the bulge develops in the dent contact region. The stress level of the contact region during initial pressurization is in a state of plastic tension. Removal of the pressure puts the contact region in a state of plastic compression from the reversal of bending stress as the dent depth increases to the final residual depth. After initial and final rebound, the length of pipe affected with residual stress is approximately one pipe diameter (18 in.) from the center of the dent.

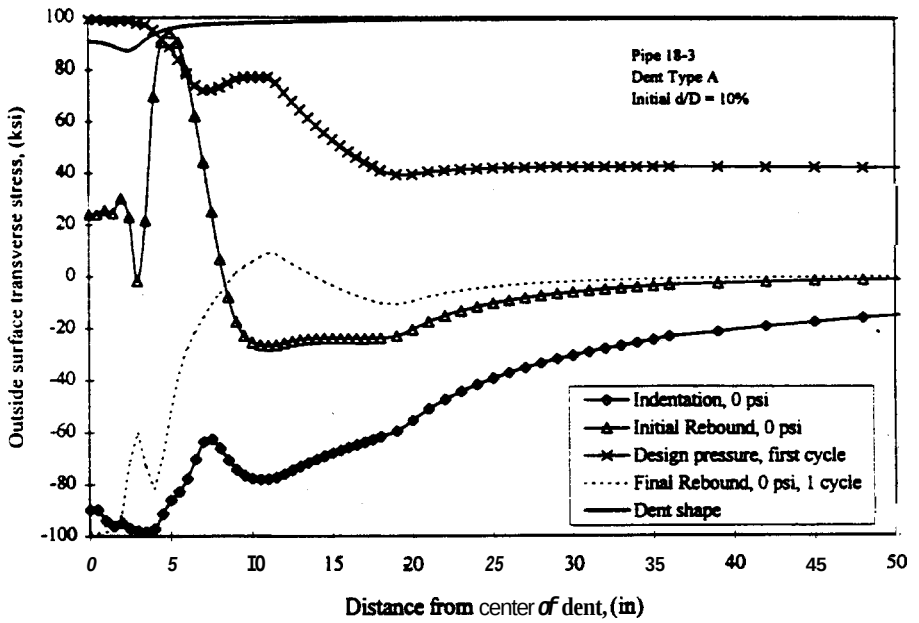

Figure 4-65: Outside surface transverse stress behavior from indentation through final rebound for Pipe 18-3 with a 10 percent *d/D*, Type A dent.

After rebound to the final residual dent depth was achieved, the model was pressure cycled such that equilibrium of the state of stress at zero pressure remained with additional

pressure cycling. Afterwards, the pressure was incrementally increased up to the design pressure to give stress range data. The stress data was recorded at different pressures based on the percentage of the pressure to cause the membrane hoop stress to reach the yield stress (percent yield pressure). The yield stress modeled for Pipe 18-3 is for grade X60 pipe (60 ksi). The corresponding design membrane hoop stress is 42 ksi. The stress distribution for Pipe 18-3 with the 10 percent *d/D* Type A dent is given in Fig. 4-66. This dent exhibits Mode 1 failure in the contact region at the center of the bulge. With zero internal pressure, the dent contact region is in a state of plastic compression as in Fig. *4-65.* At 20 percent of the yield pressure, the outside surface transverse stress reaches a stress state near equilibrium at the center of the dent. *An* increase to 40 percent of the yield pressure puts the center of the bulge in a state of plastic tension. The increase of 20 percent of the yield pressure corresponds to an increase in hoop membrane stress of 12 ksi. The increase of transverse stress is approximately 80 ksi, which gives a stress concentration factor of 6.7 between the pressure levels of 20 percent and 40 percent yield pressure. Additional pressurization puts the entire contact region in a state of plastic tension. At a distance of one pipe diameter from the center of the dent, the stress values are near the values of the membrane hoop stress.

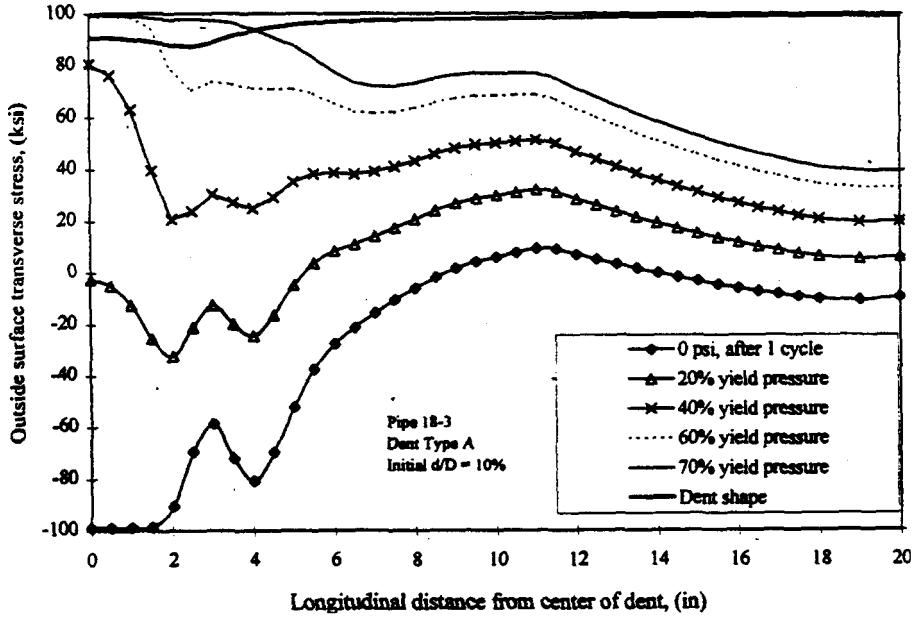

Figure 4-66: Outside surface transverse stress behavior during pressure cycling for Pipe 18-3 with a 10 percent *d/D* Type A dent.

Outside surface transverse stress contour plots are given for the 10 percent d/D Type A dent in Pipe 18-3 in Fig. 4-67 and 4-68 at zero pressure and at the design pressure. At zero pressure, the transverse stress in the contact region is in a state of compressive stress beyond the yield stress. The transverse stress outside of the contact region is in the elastic range. At the design pressure, the contact region is in a state of tensile stress beyond the yield stress. High compressive stresses are located approximately 30 degrees away from the dent along node set RING1. This region remains in compression throughout pressure cycling.

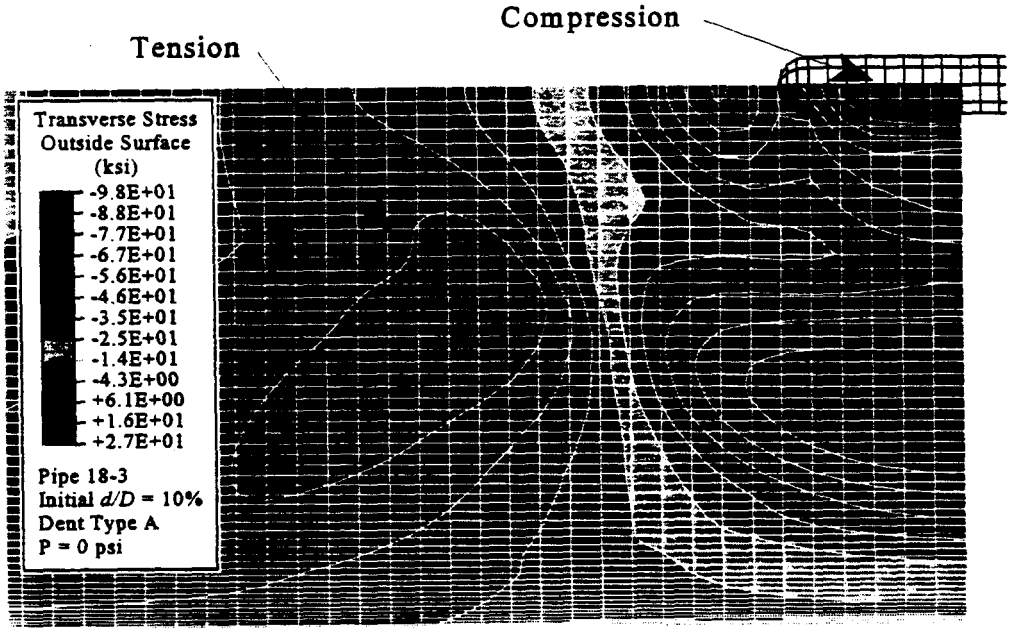

Figure 4-67: Outside surface transverse stress contour plot for Pipe 18-3 with a 10 percent d/D Type A dent at 0 psi.

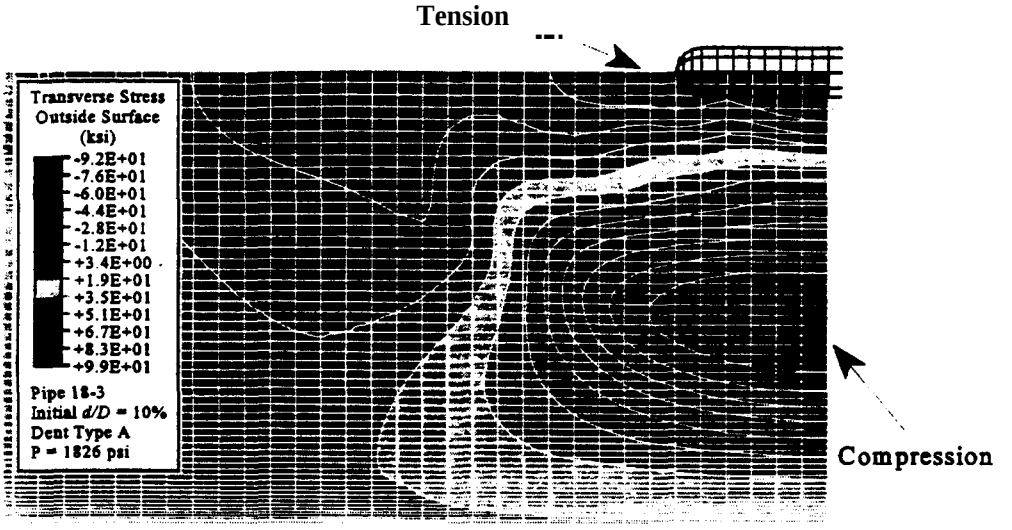

Figure 4-68: Outside surface transverse stress contour plot for Pipe 18-3 with a 10 percent *d/D* Type A dent at the design pressure.

The stress distribution of the dent contact region given in Fig. 4-66 is caused by bending stress caused fiom pressurization. There are no significant stress concentrations caused by the fluctuation of membrane stress alone. The averaged thru-thickness stress distribution for Pipe 18-3 with the 10 percent *d/D* Type A dent is given in Fig. 4-69. The average of the surface stresses gives a representation of the membrane stress. The largest stress range is located in the periphery of the dent contact region approximately 2 in. away from the end of the contact area. This peripheral location has less deformation than the contact region, thus making the contact region more flexible. Strain compatibility causes some membrane hoop stress to flow around the contact region, thus creating the peripheral membrane stress concentration. This membrane stress concentration exists, but is insignificant as compared to the stress concentration on the outside surface due to bending.

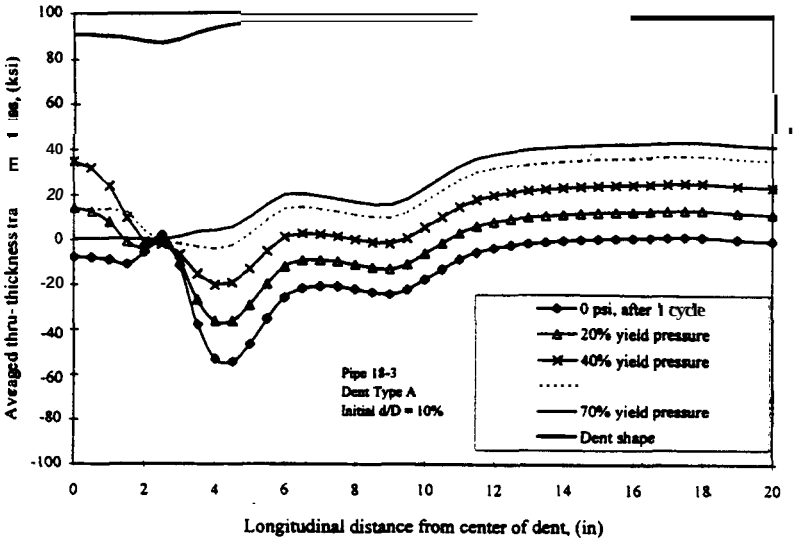

Figure *4-69:* Averaged thru-thickness transverse stress behavior during pressure cycling for Pipe **18-3** with a **10** percent *d/D* **Type** A dent.

Dent depth influences the outside surface transverse **stress** distribution. The stress distributions for Pipe **18-3** with the **5** percent and **15** percent *d/D* **Type** A dents **are** given in Figs. **4-70** and **4-71,** respectively. The **5** percent *d/D* dent does not have enough dent depth ***to*** cause a noticeable bulge unlike the deeper dents. All tbree dent depths have similar **stress** ranges **from** zero pressure to the design pressure during pressure cycling **as** shown in Fig. 4-72. The **5** percent *d/D* dent **has** the most **gradual stress** distribution. The **15** percent *d/D* dent **has high** stress values at the center of the dent like the other dent depths, but it **has** a noticeable reduction in stress at the end of the dent contact region. The increased dent depth increases the stiffness at the end of the contact region which **reduces** the bending **stress** concentration. **Based** on stress range **data** alone, the three dents of different depth would have similar fatigue lives. Fatigue life **data** from the experimental program **will** show that deeper **Type** A dents in pipes with dimensions **similar** to that of Pipe **18-3** have significantly lower fatigue lives **as** compared to shallow **dents. Thus,** the fatigue life of Pipe **18-3** cannot be based strictly on stress range **data.** A damage term based on dent depth and contact damage needs to be factored into a fatigue life prediction method. These two parameters influence the 'residual **stress** distribution **and,** thus, fatigue behavior.

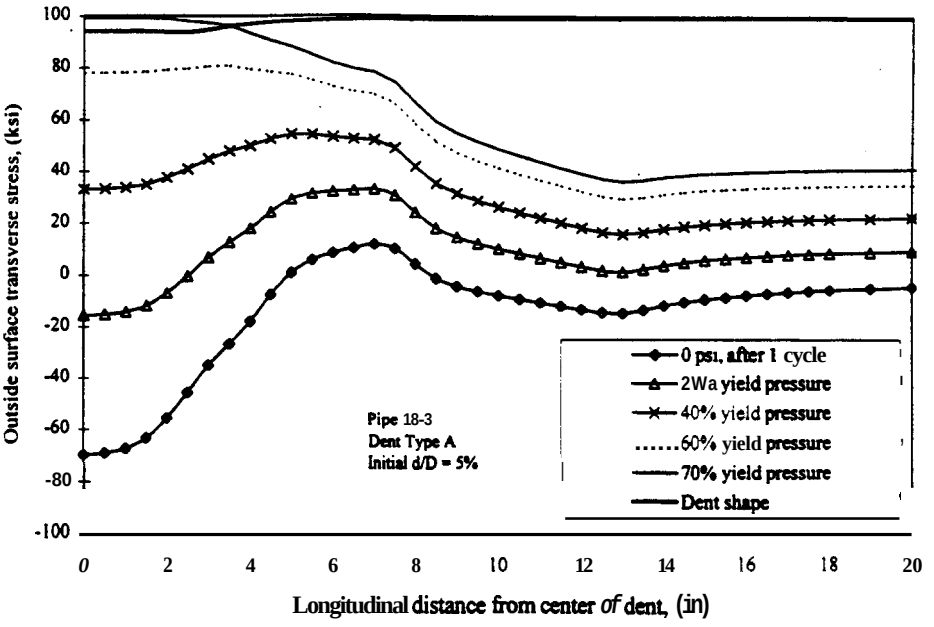

Figure 4-70: Outside surface transverse stress behavior during pressure cycling for Pipe 18-3 with a 5 percent *d/D* Type A dent.

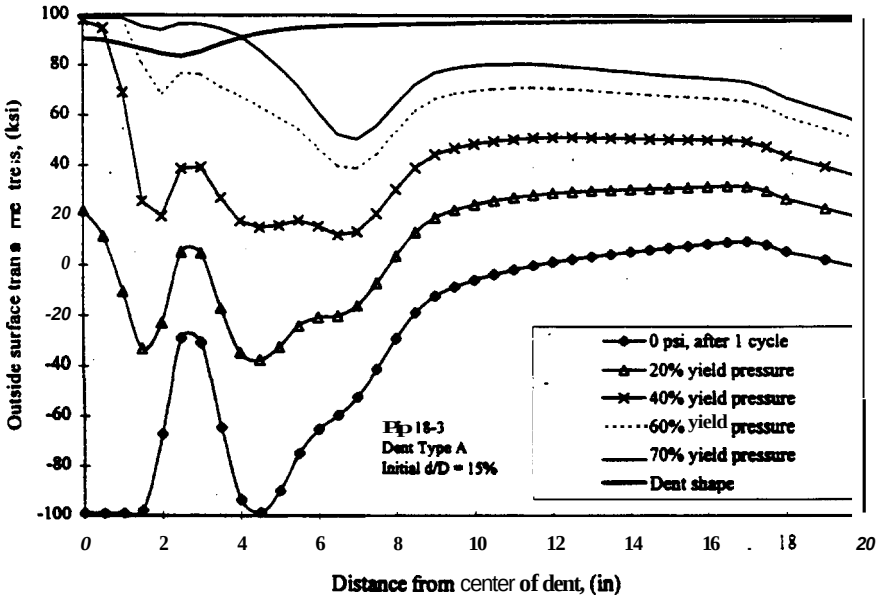

Figure 4-71: Outside surface transverse stress behavior during pressure cycling for Pipe 18-3 with a 15 percent *d/D* Type A dent.

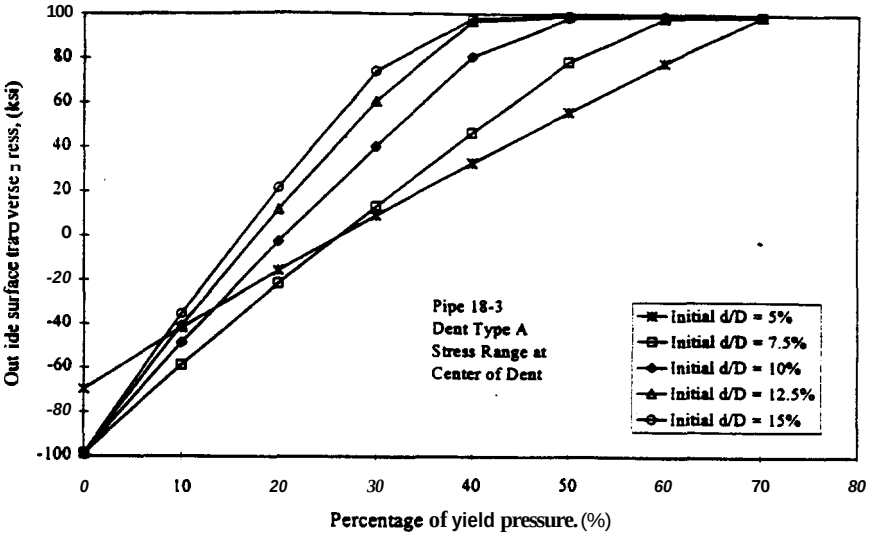

Figure 4-72: Stress Range during Pressure Cycling for Pipe 18-3 with Type A dents.

Unrestrained longitudinal Type A dents in pipes with diameters ranging up to 30 in. show similar stress distributions as in Pipe 18-3 causing Mode 1 failure at the center of the contact region. A transition in failure mode fiom Mode 1 to Mode 2 occurs for Type A dents. The parameters affecting the transition of failure mode include:

- Diameter
- Thickness
- Dent Depth.

Mode 2 failures only occur in large diameter pipes. Thicker pipes exhibit failure Mode 2. Increasing dent depth increases the dent stiffness which also leads to failure Mode 2.

The mode of failure is easily predicted by viewing the outside surface transverse stress distribution. The stress distributions for Pipe 30-3 with the 5, 10, and 15 percent d/D Type A dents are given in Figs. 473, 474, and 475, respectively. Pipe 30-3 has a slenderness ratio (D/t) of 80. The stress distribution for the percent d/D dent for Pipe 30-3 has a similar stress

distribution as the 5 percent d/D dent for Pipe 18-3 with the maximum stress range at the center of the dent. This shallow dent in Pipe 30-3 will have a Mode 1 failure in the center of the dent. The stress distribution for the 10 percent d/D dent for Pipe 30-3 has a significantly different stress distribution when compared to the 5 percent d/D dent. The highest stress range for the 10 percent d/D dent is located in the periphery of the dent.

The stress range at the center of the 10 percent d/D dent is lower than for the 5 percent d/D dent. A further reduction of the stress range occurs with an increase in initial dent depth to 15 percent d/D. The 10 percent d/D and 15 percent d/D Type A dents in Pipe 30-3 are expected to have Mode 2 failure corresponding to development of periphery cracks outside the dent contact region. Damage in the contact area from indentation might cause Mode 1 failures for the two deeper dents. Contact damage was not modeled and is excluded in influencing the failure modes.

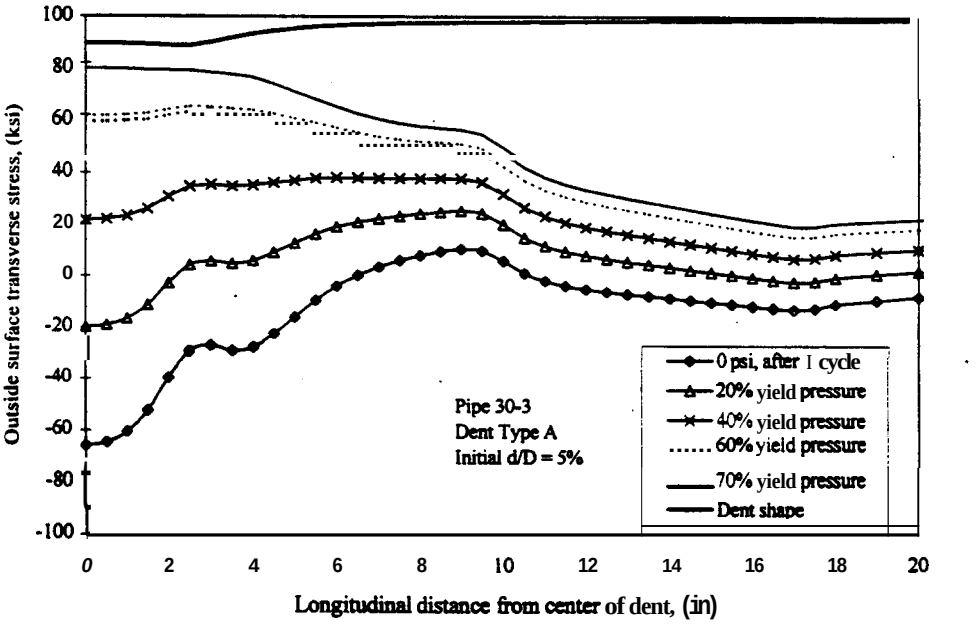

Figure 4-73: Outside surface transverse stress behavior during pressure cycling for Pipe 30-3 with a 5 percent d/D Type A dent.

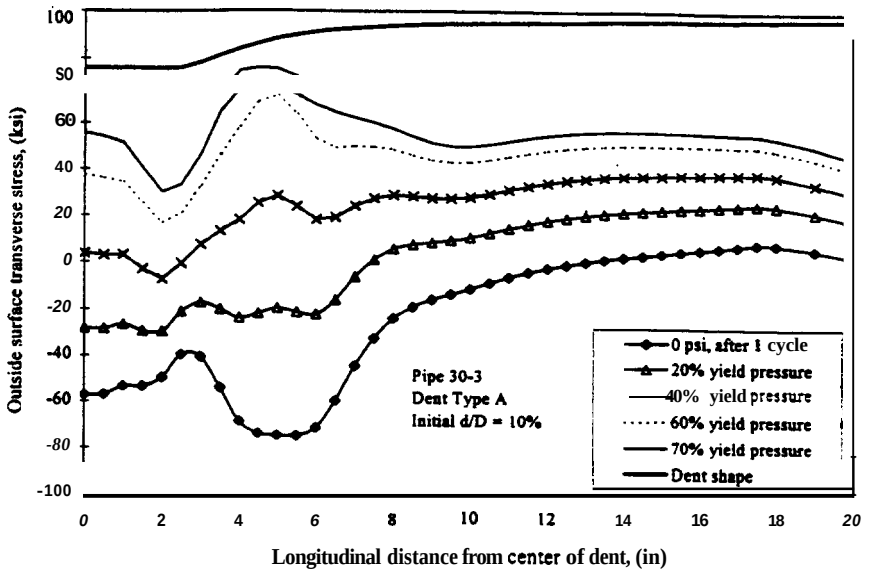

Figure 4-74: Outside surface transverse stress behavior during **pressure cycling for Pipe 30-3** with **a 10 percent** *d/D* Type **A dent.**

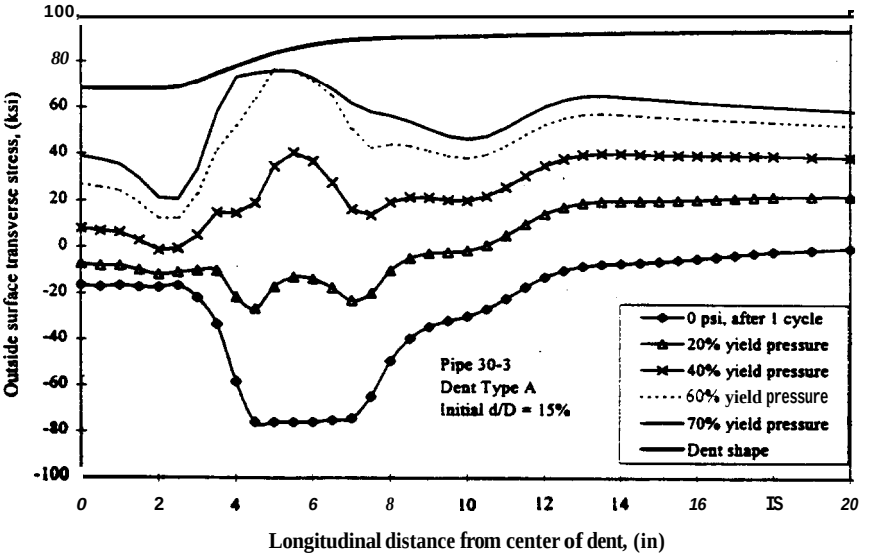

Figure 4-75: Outside surface transverse stress behavior during pressure cycling for Pipe 30-3 with a 15 percent *d/D* Type **A dent.**

The transition **in failure modes in Pipe 30-3** with **unrestrained longitudinal** Type **A dents**

is caused by the increase in dent stiffness related to an increase in dent depth. The increased stiffness reduces the bending stress that develops in the contact region. The increase in dent depth influences the membrane stress distribution in the dented region. The averaged *thru*-thickness stress distributions for Pipe 30-3 with 5 and 10 percent *d/D* Type A dents are given in Figs. 4-76 and 4-77. For the 5 percent *d/D* dent, the averaged thru-thickness stress range represents the increase in membrane stress from pressurization. The stress range is near zero at the end of the contact location, which causes a slight stress concentration of membrane stress in the dent periphery. The averaged thru-thickness stress range for the 10 percent *d/D* dent is considerably different from that of the 5 percent *d/D* dent. For the 10 percent *d/D* dent, the stress range is near zero for the entire contact region of the dent. A stress range of approximately 60 ksi is located in the dent periphery. The periphery of the dent has a membrane stress concentration since the membrane stress flows around the dented region. This can be related to the stress distribution of a hole in a plate loaded in tension. For the plate, the stress must flow around the hole causing a stress concentration on both sides of the hole. The dented region acts similar to the hole causing a stress concentration on both sides of the dented region.

The transition of failure mode from Mode 1 to Mode 2 for Pipe 30-3 influences the fatigue life. In the experimental program, dents with Mode 1 failures had considerably lower fatigue lives as compared to dents with Mode 2 failures. This is attributed to the fact that Mode 1 failures occur in the damaged contact area, unlike Mode 2 failures which occur outside the contact region in the undamaged periphery of the dent. For Pipe 30-3, the predicted failure modes for dent depths of 5, 10, and 15 percent *d/D* were Modes 1, 2, and 2, respectively. The fatigue life of the 5 percent *d/D* dent will likely have the shortest fatigue life since it will have a Mode 1 failure. Increasing the dent depth suppresses Mode 1 failure leading to Mode 2 failure. The change in failure mode will likely make the two deeper dents have longer fatigue lives than the shortest dent. The 15 percent *d/D* dent will have a longer fatigue life than the 5 percent *d/D* due to transition of failure mode, but it will have a shorter life than the 10 percent *d/D* since they both have the same Mode 2 failure. Thus, for Pipe 30-3 with Type A dents, deeper dents may have longer fatigue lives than shallow dents.

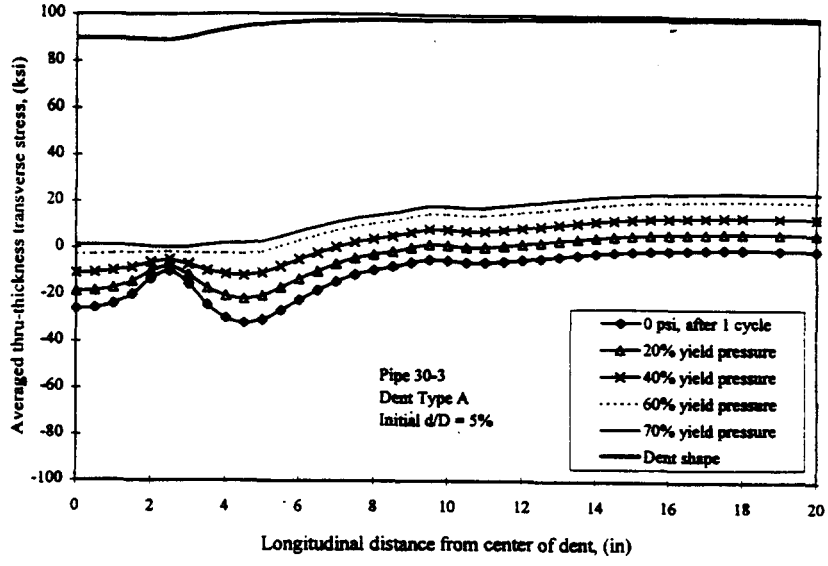

Figure 4-76: Averaged thru-thickness transverse stress behavior during pressure cycling for Pipe **30-3** with **a 5 percent** *d/D* Type **A dent.**

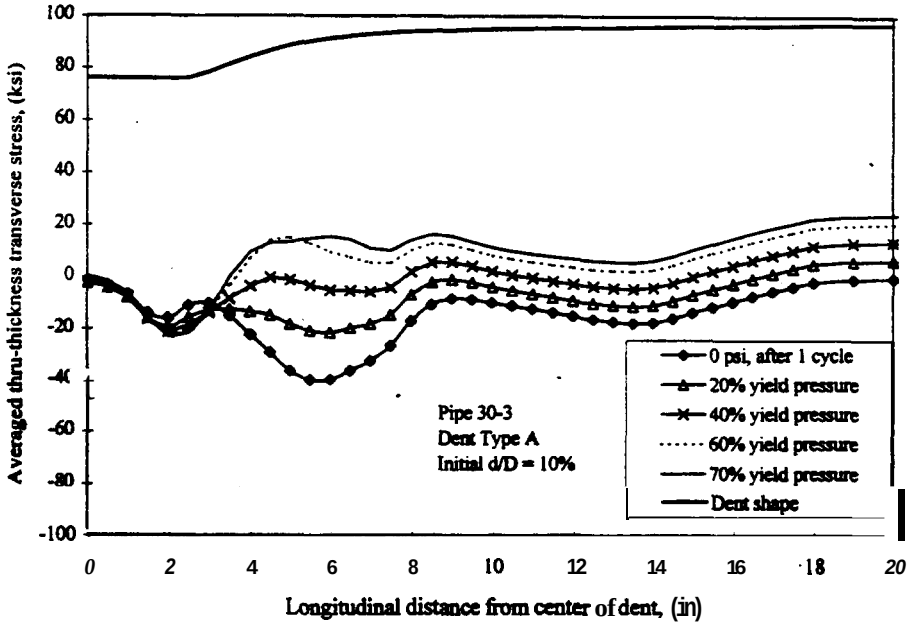

Figure 4-77: Averaged thru-thickness transverse stress behavior during pressure cycling for Pipe 30-3 with **a 10 percent** *d/D* **Type A dent.**

The study of the transverse outside surface stress of unrestrained longitudinal Type A dents for the parameters of diameter, thickness, and dent depth will show the influence of the parameters on the failure mode of a specific dent. Table 4-11 shows the predicted failure modes of the unrestrained longitudinal Type A dents modeled. Type A dents in the smaller diameter pipes tend to have Mode 1 failures regardless of thickness and dent depth. Larger diameter pipes have both modes of failure which are influenced by thickness and dent depth.

Table 4-11: Unrestrained Longitudinal Dent Type A Predicted Failure Modes.

Diameter (in)	Thickness (in)	Initial d/D (%)				
		5	7.5	10	12.5	15
12	0.250	1	1	1	1	1
12	0.375	1	1	1	1	1
12	0.500	1	1	1	1	1
18	0.250	1	1	1	1	1
18	0.375	1	1	1	1	1
18	0.500	1	1	1	1	1
24	0.250	1	1	1	1	1
24	0.375	1	1	1	1	1
24	0.500	1	1	1	1	1, 2
24	0.625	1	1	1	1, 2	2, 1
30	0.250	1	1	1	1	1, 2
30	0.375	1	1	2, 1	2	
30	0.500	1	1, 2	2	2	2
30	0.625	1	1, 2	2	2	2
30	0.750	1	1, 2	2	2	2
36	0.250	1	1	1	1	1, 2
36	0.375	1	1, 2	2, 1	2, 1	2, 1
36	0.500	1	1	1, 2	1, 2	1, 2
36	0.625	1	2, 1	2	2	2
36	0.750	1	2, 1	2	2	2
48	0.375	1	1	2, 1	2, 1	2
48	0.500	1	2, 1	2	2	2
48	0.625	1	2, 1	2	2	2
48	0.750	1	2	2	2	2

Modes 1 and 2 represent long and short dent behavior, respectively.
If both are given, the most probable mode of failure is listed first.

4.5.3 Dent Type BH Stress Behavior

Unrestrained longitudinal Type BH dents behave as short dents with Mode 2 fatigue failures. All failures of Type BH dents in the experimental program were caused by peripheral cracking outside the dent contact area. Failures only occurred for Type BH dents with an initial dent depth of at least 10 percent d/D. Shallower dents did not fail or develop any peripheral fatigue cracks.

As with the Type A dent, indentation causes high compressive stress on the outside surface in the dented region with corresponding tensile stress on the inside surface due to bending stress. Figure 4-78 shows a plot of outside surface transverse stress from indentation thru final rebound for a 10 percent d/D Type BH dent in Pipe 18-3. The highest compressive stress during indentation is located at the end of the contact region. After initial rebound, the highest tensile stress is located in the dent periphery approximately 2 in. away from the end of the contact region. This high peripheral stress remains during pressurization of the first pressure cycle. Removal of the internal pressure causes a stress reversal such that the stress at the periphery is in a state of plastic compression. The maximum stress range for the Type BH during initial and final rebound is located in the dent periphery unlike the maximum stress range for the Type A dent which is located in the center of the contact region (Fig. 4-65). As with the Type A dent, the length of pipe affected with residual stress is approximately one pipe diameter (18 in.).

The stress distribution for Pipe 18-3 with the 10 percent d/D Type BH dent during pressure cycling is given in Fig. 4-79. The maximum stress range is located in the periphery of the dent at a distance of 1.5 in. from the end of the dent contact region. During pressure cycling, the contact region has a stress range located in the elastic range. The stress distribution for this dent will result in a Mode 2 fatigue failure. As with the 10 percent d/D Type A dent (Fig. 4-66), the stress values at a distance of one pipe diameter fiom the center of the dent for the Type BH dent are near the values of membrane hoop stress fiom pressurization.

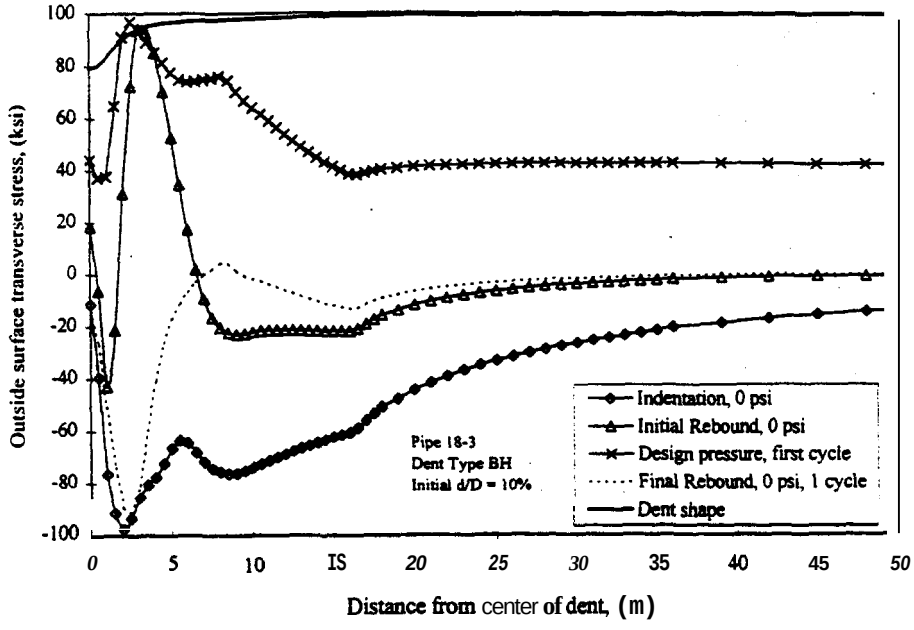

Figure 4-78: Outside surface transverse stress behavior form indentation through final rebound for Pipe 18-3 with a 10 percent d/D Type BH dent.

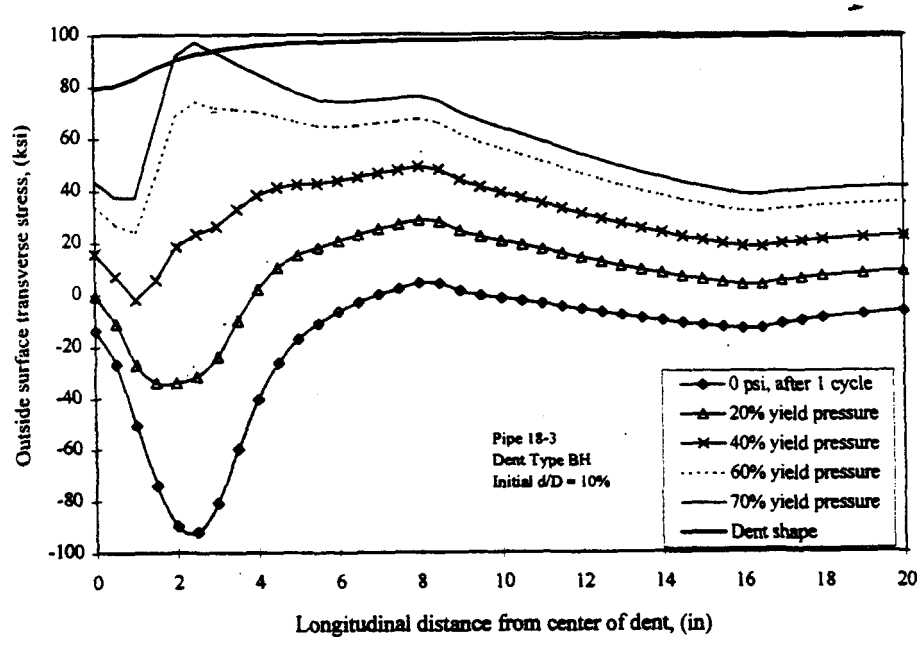

Figure 4-79: Outside surface transverse stress behavior during **pressure** cycling for Pipe 18-3 **with a** 10 percent *d/D* **Type** BH dent.

Outside surface transverse stress contour plots are given for the 10 percent *d/D* Type BH dent in Pipe 18-3 in Figs. 4-80 and 4-81 at zero pressure and at the design pressure. At zero pressure, the transverse stress in the dent periphery is in a state of compressive stress beyond the yield stress. The transverse stress in all other regions is in the elastic range. At the design pressure, the peripheral region is in a state of tensile stress beyond the yield stress. The contact region is in a state of tensile stress well below the yield stress in the elastic range.

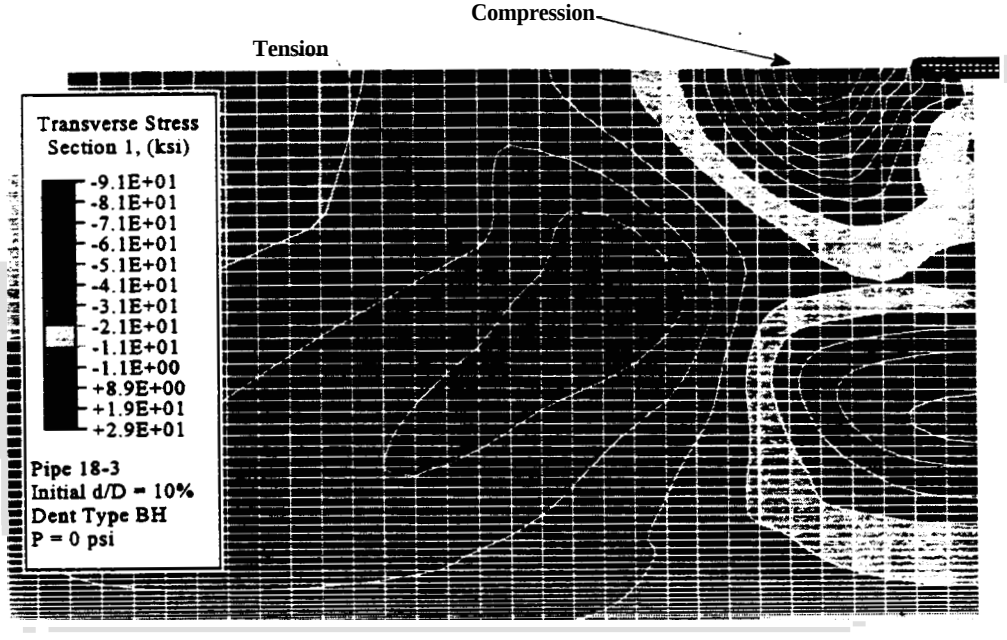

Figure 4-80: Outside surface transverse stress contour plot for Pipe 18-3 with a 10 percent *d/D* Type BH dent at 0 psi.

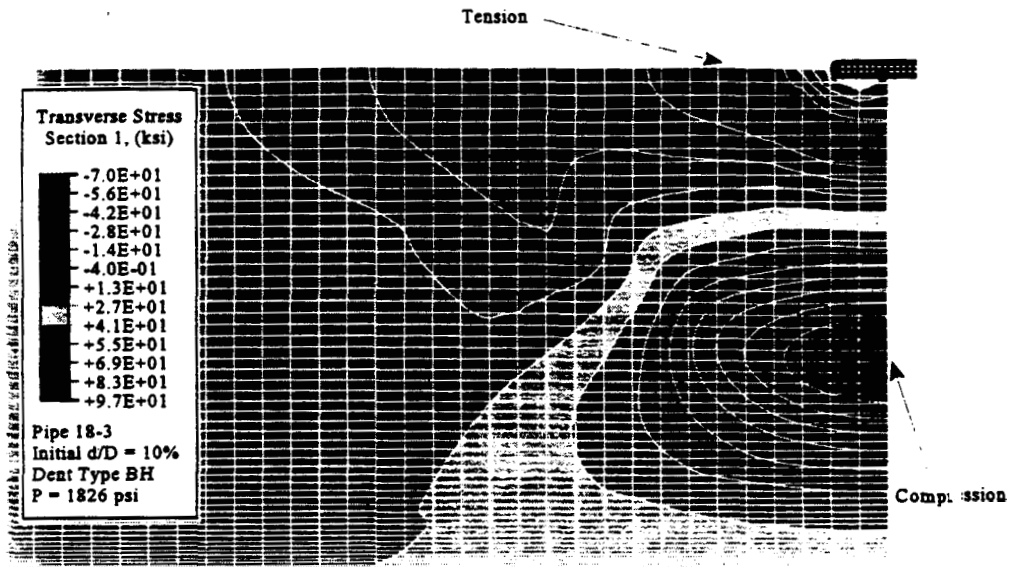

Figure 4-81: Outside surface transverse stress contour plot for Pipe 18-3 with a 10 percent d/D Type BH dent at the design pressure.

The dent depth of unrestrained longitudinal dents was found to correlate with the fatigue life of a dent in the experimental program. An increase in dent depth causes a decrease in fatigue life. The stress distributions for Pipe 18-3 with the 5, 7.5, and 15 percent d/D Type BH dents are given in Figs. 4-82,483, and 4-84, respectively. The stress distribution of the 5 percent d/D Type BH dent is similar to distributions of Type A dents which have Mode 1 failure in the dent contact region. Since no failures occurred in shallow Type BH dents in the experimental program, Mode 1 failures will be assumed to not occur in any of the Type BH modeled. By increasing the dent depth fiom 5 percent d/D to 7.5 percent d/D, the stress distribution transitions fiom Mode 1 behavior to Mode 2 behavior. The increase in dent depth reduces the stress range in the contact area and increases the stress distribution in the dent periphery. This behavior is evident with the increase of dent depths from 5 to 15 percent d/D. The stress range for the 15 percent d/D dent is near zero at the dent contact region with the maximum stress range in the dent periphery.

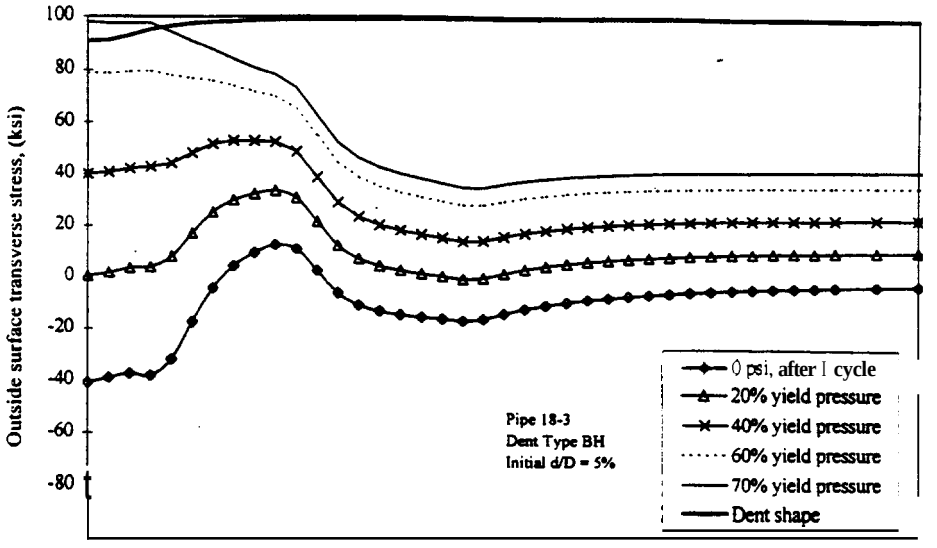

Figure 4-82: Outside surface transverse stress behavior during pressure cycling for Pipe 18-3 with a 5 percent *d/D* Type BH dent.

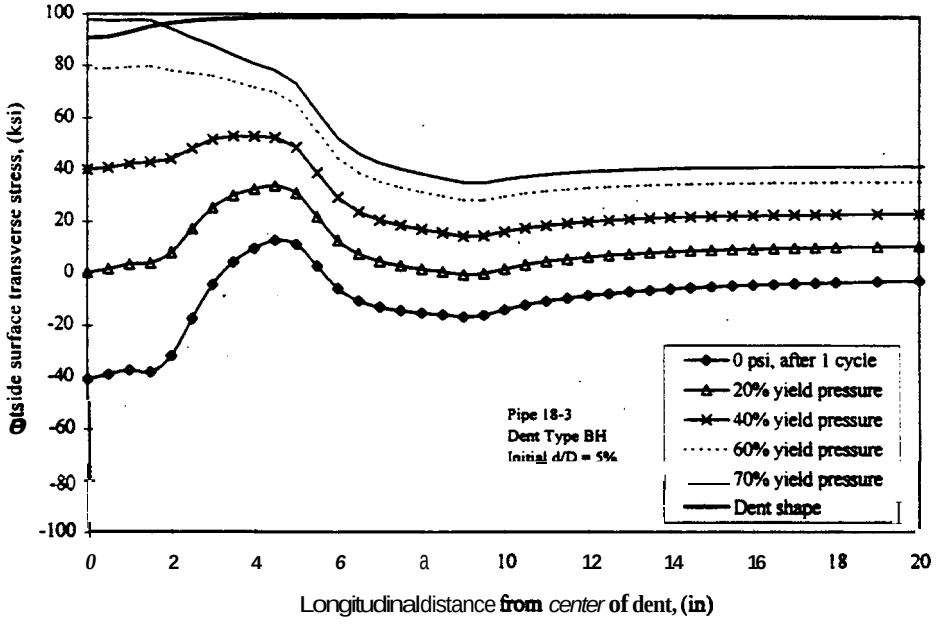

Figure 4-83: Outside surface transverse stress behavior during pressure cycling for Pipe 18-3 with a 7.5 percent *d/D* Type BH dent.

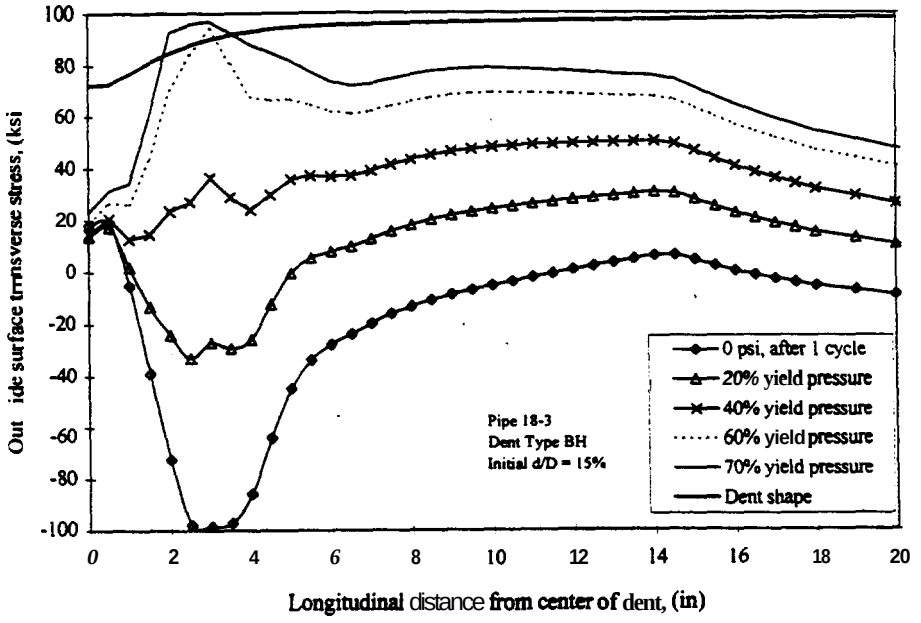

Figure 4-84: Outside surface transverse stress behavior during pressure cycling for Pipe 18-3 with a 15 percent *d/D* Type BH dent.

The location of the maximum peripheral stress range for the Type BH dents in Pipe 18-3 changes slightly based on dent depth. The location of the maximum stress range for the 7.5 percent *d/D* dent is 2.0 in. from the center of the dent, whereas the location of the maximum stress range for the 15 percent *d/D* dent is at 3.0 in. The location of maximum peripheral stress is farther away from the dent contact region for deeper dents. This is caused by the distribution of membrane stress for the different dent depths.

The membrane stress flows around the dented region as discussed with Fig. 4-63. The size of the dented region is directly related to the dent depth. As the size of the dented region increases, the maximum peripheral membrane stress range increases, and its location moves further away from the indenter contact area. This is shown with graphs of the averaged thru-thickness transverse stress. The averaged thru-thickness transverse stress distributions for Pipe

18-3 with 5, 10, and 15 percent *d/D* Type BH dents are given in Figs. 4-85, 4-86, and 4-87. The stress range increases in magnitude with increasing depth due to the increase in size of the dented area. The locations of the highest stress ranges for the 5, 10, and 15 percent *d/D* dents are at distances of 2.0 in., 2.5 in., and 3.5 in. away from the centers of the dents.

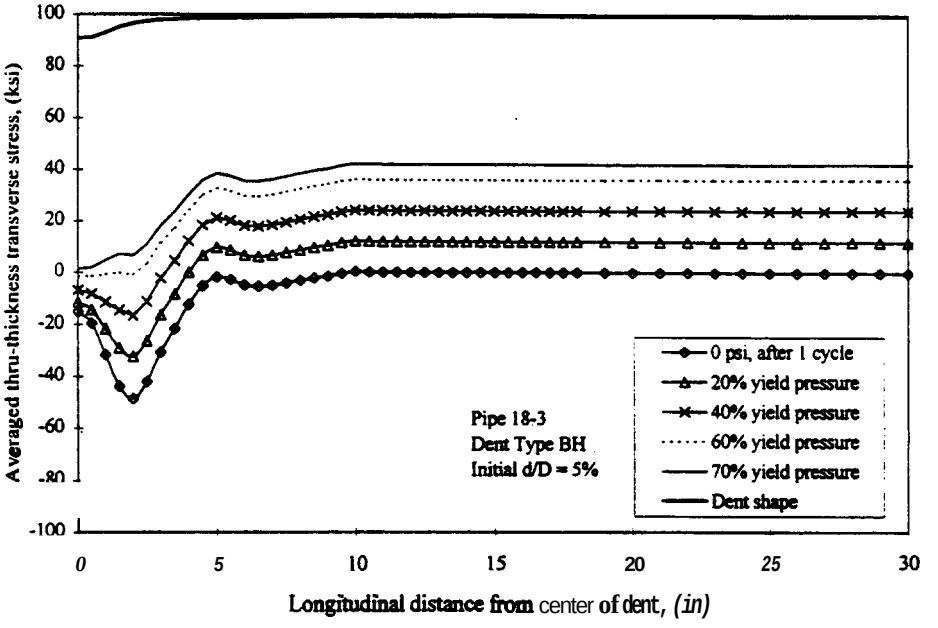

Figure 4-85: Averaged thru-thickness transverse stress behavior during pressure cycling for Pipe 18-3 with a 5 percent *d/D* Type BH dent.

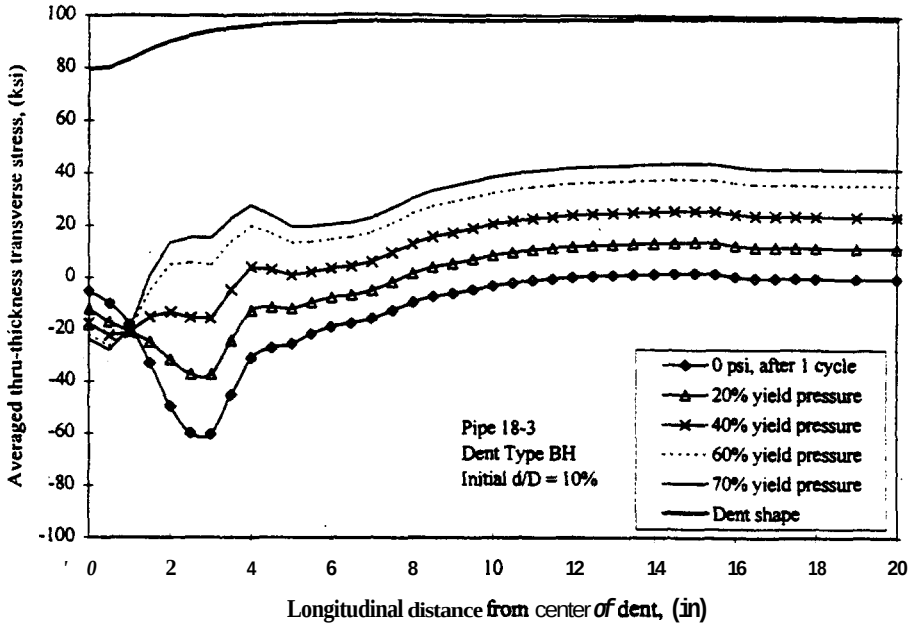

Figure 4-86: Averaged thru-thickness transverse stress behavior during pressure cycling for Pipe 18-3 with a 10 percent *d/D* Type BH dent.

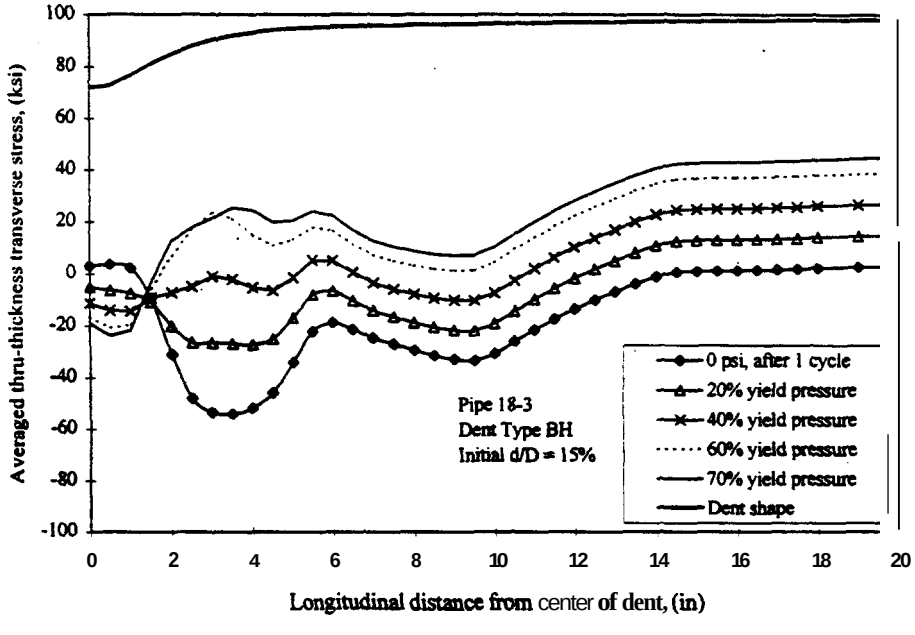

Figure 4-87: Averaged thru-thickness transverse stress behavior during pressure cycling for Pipe 18-3 with a 15 percent *d/D* Type BH dent.

All Type BH dents in different pipe sizes have similar stress distributions of outside surface transverse at Pipe 18-3. The location of the maximum outside surface peripheral stress range from the center of the dent is influenced by dent depth, diameter, and thickness. An increase in any of the parameters will cause an increase in the length from the center of the dent of the maximum stress range. An example of the influence of diameter is shown by comparing Pipes 18-3 and 30-3 with similar dent depths. The stress distribution for Pipe 30-3 with the 10 percent *d/D* Type BH dent during pressure cycling is given in Fig. 4-88. The location of the maximum stress range for the 10 percent *d/D* Type BH in Pipe 30-3 is 4.0 in. away from the center of the dent. The similar location for the 10 percent *d/D* Type BH in Pipe 18-3 (Fig. 4-79) is only 2.5 in. away from the center of the dent. Thus the failure location shifts, but the mode of failure remains the same.

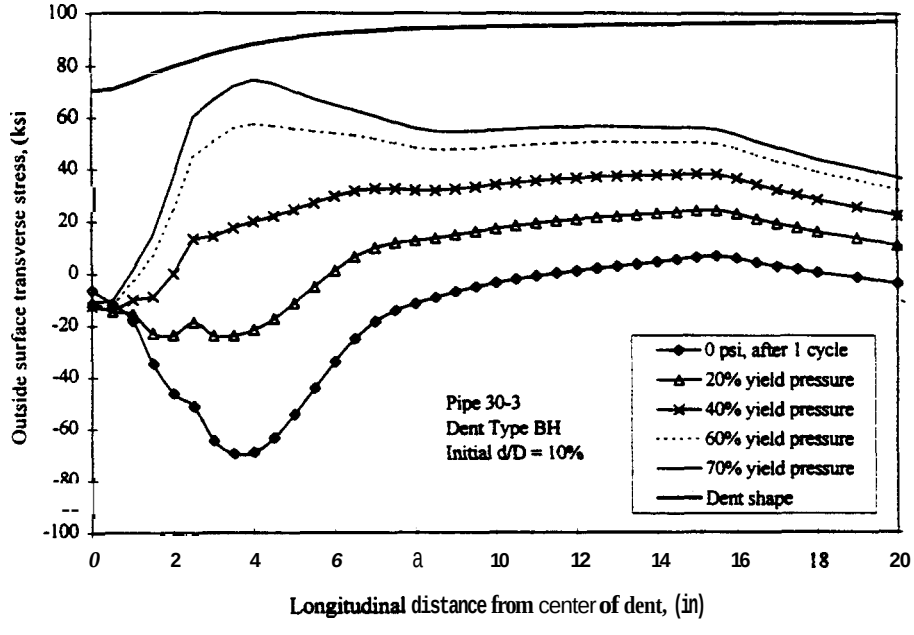

Figure 4-88: Outside surface transverse stress behavior during pressure cycling for Pipe 30-3 with a 10 percent *d/D* Type BH dent.

The study of transverse outside surface stress of unrestrained longitudinal Type BH dents for the parameters of diameter, thickness, and dent depth shows no change in fatigue failure behavior. Table 4-12 shows the predicted failure modes of the unrestrained longitudinal Type

BH dents modeled. The shallow 5 percent *d/D* dents for diameters up to 24 in. gave stress distributions which suggest long dent behavior, and the failure modes were predicted based on that. The experimental program did not have any failures below 10 percent *d/D* for Type BH dents, thus, the 5 percent *d/D* dents with Mode 1 stress distributions for Type BH dents should be acceptable in pipelines regardless of the predicted failure mode. Compressive residual stresses associated with the contact damage prevent Mode 1 failures in shallow Type BH dents. Modeling with shell elements does not account for the localized contact damage which suppresses failure Mode 1.

Table 4-12: Unrestrained Longitudinal Dent Type BH Predicted Failure Modes.

Diameter (in)	Thickness (in)	Initial d/D (%)				
		5	7.5	10	12.5	15
12	0.250	1	2	2	2	2
12	0.375	1	2	2	2	2
12	0.500	1	2	2	2	2
18	0.250	1	2	2	2	2
18	0.375	1	2	2	2	2
18	0.500	1	2	2	2	2
24	0.250	1	2	2	2	2
24	0.375	1	2	2	2	2
24	0.500	1	2	2	2	2
24	0.625	1	2	2	2	2
30	0.250	2	2	2	2	2
30	0.375	2	2	2	2	2
30	0.500	2	2	2	2	a
30	0.625	2	2	2	2	2
30	0.750	2	2	2	2	2
36	0.250	2	2	2	2	2
36	0.375	2	2	2	2	2
36	0.500	2	2	2	2	2
36	0.625	2	2	2	2	2
36	0.750	2	2	2	2	2
48	0.375	2	2	2	2	2
48	0.500	2	2	2	2	2
48	0.625	2	2	2	2	2
48	0.750	2	2	2	2	2

Modes 1 and 2 represent *long* and short dent behavior, respectively.
If both are given, the most probable mode of failure is listed first.